Polymer 51 (2010) 1954–1963

Contents lists available at ScienceDirect

Polymer

journal homepage: www.elsevier.com/locate/polymer

Contribution of physico-chemical properties of interfaces on dispersibility, adhesion and flocculation of filler particles in rubber

Klaus Werner Stöckelhuber*, Amit Das, René Jurk, Gert Heinrich

Leibniz-Institut für Polymerforschung Dresden e.V., Hohe Str. 6, D-01069 Dresden, Germany

ARTICLE INFO

Article history:
Received 11 May 2009
Received in revised form
28 February 2010
Accepted 4 March 2010
Available online 15 March 2010

Keywords:
Rubber nanocomposites
Surface energy
Filler flocculation

ABSTRACT

Reinforcing fillers are added to elastomeric compounds to improve and adjust several mechanical, dynamical, tribological, etc. properties with respect to different applications, i.e. for automotive tires, or technical rubber goods. Carbon black and precipitated silica are widely used as rubber reinforcing fillers; however, some new classes of nanosized substances like organophilic modified clay or carbon nanotubes are presently intensive studied as possible future filler systems in combination with carbon black or silica.

An important parameter for the dispersibility and compatibility of the filler in the polymer matrix of rubber compounds is the surface energy and surface polarity of the solid filler particles. Therefore, we systematically measured and compared the dynamic contact angles of a collection of different filler types (carbon blacks, silica, carbon nanotubes and organoclays) using the Wilhelmy method, whereby the particles were fixed as a thin layer at a double-sided adhesive tape. From the contact angle values the polar and disperse part of the surface energies of the filler particles were calculated by fitting Fowkes formula. For an estimation of the compatibility of the fillers with different types of rubber polymers we additionally analyzed the surface energy and polarity of the gum (unfilled) elastomers. From the evaluated surface energies and polarities, thermodynamic predictors for the dispersibility (enthalpy of immersion), the adhesion between filler particles and polymer matrix in the nanocomposite, and for the flocculation behaviour of the particles in a rubber matrix (difference in the works of adhesion) were derived. These thermodynamic predictors improve considerably the compounding process of novel rubber nanocomposites with respect to target-oriented adjustment of rubber properties.

1. Introduction

The performance of elastomeric materials is significantly affected by the reinforcing filler dispersed therein. Nearly no rubber material, i.e. car tire treads, is produced without the addition of nanostructure filler particles [1]. The first reinforcing filler was carbon black, which has been replaced in the last decade in passenger car tires more and more by precipitated silica in combination with a corresponding coupling agent. The silica technology allows better adjusted dynamic-mechanical properties, i.e. a lower rolling resistance resulting in lower fuel consumption (the so-called green tyre). Based on the successful implementation of the silica system, novel nanoscale filler materials for elastomers are now in consideration, like carbon nanotubes and organophilic modified clay minerals [2–4].

A main problem in the implementation of the new filler materials is the dispersibility of the filler particles in the rubber matrix. An often neglected issue in rubber technology is hereby the surface energy of the filler particle surface, which is determining the wetting of the filler by the rubber polymers.

Knowing the surface energy (and polarity) of the filler and the surface tension of the used rubber polymer, it should be possible to predict the dispersibility of the filler particles in this elastomer; or, to say it more precisely, the thermodynamic contribution of the wetting step on the dispersion process. In the case of silica, a surface modification by the use of silanes is state of the art; this processing step leads to a better dispersibility and, additionally, to the formation of chemical linkages between filler and polymer during the crosslinking reactions (vulcanization) [5].

Interfacial forces between filler and elastomeric matrix, which are a result of the surface energies of filler particles and polymers, are also important for the mechanical properties of the resulting composites. Hereby, the calculation of a work of adhesion value between rubber and elastomer is an useful indicator to estimate the internal adhesion between filler particle surface and rubber polymer.

In uncured rubber compounds at elevated temperature a re-agglomeration of the already dispersed filler particles is observed;

* Corresponding author.
E-mail address: stoeckelhuber@ipfdd.de (K.W. Stöckelhuber).

0032-3861/$ – see front matter © 2010 Elsevier Ltd. All rights reserved.
doi:10.1016/j.polymer.2010.03.013

this process is know as filler flocculation and leads to special non-linear dynamic-mechanical properties of the rubber compounds (the so-called Payne-effect) [6]. This process is also driven by the physico-chemical surface properties of the filler and the rubber polymer. Hereby, the difference between the work of adhesion between two adjacent filler particles and the wetted state (filler/polymer) is the driving force of filler flocculation [7].

2. Experimental

2.1. Materials

2.1.1. Fillers

For the calculation of surface energies and polarities of filler particles the following nanoscale filler systems are being used: precipitated silica (Degussa VN3 in powder and granulated form), precipitates silica, surface modified with bis(triethoxysilylpropyl) polysulfide (Coupsil 8113 in powder and Coupsil 8113GR granulated form), fumed silica (Aerosil 200, Degussa), methylated fumed silica (Aerosil R974). Carbon Blacks in different grades (N121, N339, N990, Corax grade,) were obtained from Evonik Degussa, Germany. The used layered silicate filler consist of unmodified montmorillonite (Nanofil 757, Südchemie, Moosburg, Germany) and two grades of organophilic modified grades (Nanofil 5, Nanofil 15, Südchemie, Moosburg, Germany). Carbon Nanotubes were obtained by Nanocyl, Namur, Belgium (unmodified thin multiwalled nanotubes industrial grade NC7000, hydroxy-functionalisated (NC-3153) and mercapto-functionalisated (NC-3154) thin multiwalled nanotubes, research grade).

2.1.2. Rubber polymers

For the estimation of the compatibility of the fillers and the elastomers also the surface energy and polarity of a set of rubber polymers was investigated by contact angle measurements. The following rubber polymers were tested: natural rubber (NR, TMR - Standard Malaysian Rubber SMR 20), polybutadiene rubber (BR, Lanxess Buna CB25), ethylene-propylene-diene rubber (EPDM, Lanxess Buna EP G6850), three different acrylonitrile-butadiene rubbers with different acrylonitrile content (NBR, Lanxess Perbunan 1846F, Lanxess Perbunan 3446F and Lanxess Perbunan 4456F), hydrogenated acrylonitrile-butadiene rubber (HNBR Lanxess Therban TM A3407), polychloroprene rubber (Lanxess Baypren) and carboxylated acrylonitrile-butadiene rubber (XNBR Lanxess Krynac X740).

2.1.3. Test liquids for wetting experiments

Surface energies are calculated out of the results of wetting experiments. For this purpose a set of test liquids with different surface tension (and polarity) was used: Water (Millipore Milli-Q-Quality), formamide (Merck, Darmstadt, Germany), ethylenglycol (Fisher Scientifiy, Loughborough, UK), dodecane (Merck Schuchardt, Hohenbrunn, Germany), hexadecane (Merck, Darmstadt, Germany), ethanol (Uvasol, Merck, Darmstadt, Germany) and mixtures of ethylenglycol or ethanol resp. with water(EtOH/H_2O 1 + 9 and EtGly/H_2O 2 + 8).

2.2. Experimental setup

Wetting experiments (Wilhelmy method, and capillary penetration method) were taken out, using the dynamic contact angle meter and tensiometer DCAT 21, DataPhysics Instruments GmbH, Filderstadt, Germany.

Sessile drop contact angle measurements are conducted with the automatic contact angle meter OCA 40 Micro, DataPhysics Instruments GmbH, Filderstadt, Germany.

Flocculation measurements were carried out using a moving die rheometer (Scarabaeus, Langgöns, Germany). Mixtures of a rubber polymer and the filler particles were measured at 160 °C and a pressure of 4 bar under varied shear amplitudes.

2.3. Sample preparation

For the Wilhelmy measurements the filler particles were put in a shallow plate. In the filler powder a 2 × 1 cm piece of a double-face adhesive tape (TESA 55733, Beiersdorf Germany), was immersed and gently moved, until the tape was uniformly coated by filler particles. Surplus particles, which did not stick at the adhesive tape, were blown away by a stream of nitrogen. The filler particle covered tape was used for Wilhelmy contact angle measurements without further modification.

For capillary penetration measurements a constant mass of filler (2g) was given in a glass tube, sealed at bottom by a thin semi-permeable membrane filter (Durapore 0.45μm HV, Millipore, USA). To obtain comparable packing densities, the powder in the test tubes was compacted by means of a modified tabbed density tester (100 strokes, STAV 2003, Engelsmann, Ludwigshafen, Germany). Capillary penetration measurements of the so prepared tubes were undertaken using the Dataphysics DCAT21 device.

To obtain samples of the uncured rubber polymers, the rubber was heated in a hot press for 10 min at 160 °C at a press force of 100 kN in a PTFE-coated mould to minimize surface contamination of the rubber samples. The contact angles of the plates of the so manufactured uncured rubber polymers were measured using sessile drop technique (DataPhysics OCA 40 Micro) and Wilhelmy method (DataPhysics DCAT21).

3. Results

3.1. Measurement of surface energies

3.1.1. Contact angle measurements at nanoscale particles

Contact angle measurement at granular matter is still a challenging task. For analyzing the wetting behaviour of powders, several methods are described in literature [8]. In the scope of this work a set of different filler systems are to be investigated. In all of these particle systems, the typical length scale of a primary particle or smallest aggregate is in the range of 10–100 nm. Also the geometry of the used filler systems are very different; it ranges from aggregates of spherical particles in the case of silica and carbon black, over swellable stacks of platelets for layered silicates to the felted wormlike structure of carbon nanotubes, Due to this facts, direct measurements of contact angles at the particles (like the particle interaction method or film flotation) are not possible.

The perhaps most common method for contact angle measurement of granular material is the capillary penetration technique. Hereby, the kinetics of the capillary rise of a liquid in a tube packed with the powder sample to be examined is observed. Fig. 1 gives a schematic sketch of the measurement setup. The time dependent height of the wetted zone of the powder packing $h(t)$ is given by the well known Lucas–Washburn [9,10] equation:

$$h(t)^2 = \frac{r\gamma_l \cos\theta}{2\eta_l} t \tag{1}$$

with θ the advancing contact angle of the compacted powder bed, γ_l, the surface tension, η_l the viscosity of the test liquid and r the mean capillary radius. With higher accuracy as the wetted length of the powder package, the weight increase due to the capillary penetration of the liquid can be measured. The Lucas–Washburn equation formulates for this case:

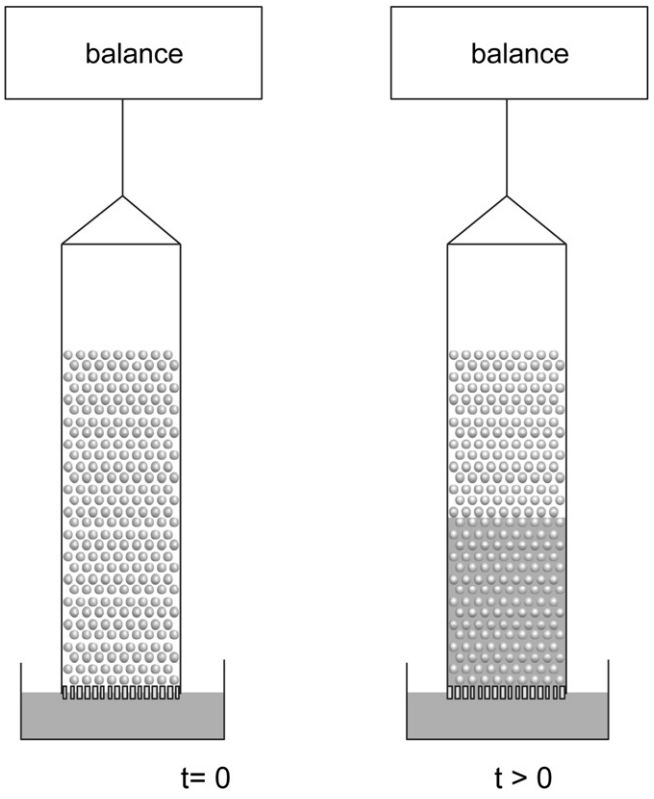

Fig. 1. Experimental setup for capillary penetration measurements. The dynamic wetting is observed by the increase of the weight of a tube filled by particles in contact with the test liquid.

$$m(t)^2 = \frac{\rho_l^2 \left[A^2 \cdot r\right] \gamma_l \cos\theta}{2\eta_l} t \qquad (2)$$

with m mass difference, ρ_l density of the test liquid and A the cross sectional area of the powder packing.

A problem in capillary penetration measurements is that the capillarity of the packed powder is unknown. Therefore, this important experimental parameter has to be measured independently by using a test liquid with low surface tension, which can be assumed as totally wetting (contact angle $\theta = 0^\circ$). After calculating the capillarity of the packed powder, the contact angle of several test liquids with different surface tension and polarities can be measured. Unmodified layered silicates showed swelling in contact with polar liquids, as organoclay with non-polar ones. Also in the case of standard fillers like silica modifications in the powder package during the capillary penetration process was observed. The same effects also occurred in contact angle measurement techniques which also require a packed powder bed, like the equilibrium capillary pressure method. Another systematic problem in capillary penetration measurements is the limitation of this technique to contact angle measurements on angle in the wetting range of 0°–90°. Due to these experimental problems these techniques could not be used for a complete comparison of all investigated filler systems, even if these methods are working reliably on a part of filler types, which do not exhibit swelling or deagglomeration phenomena.

A different approach to measuring contact angles of granular materials is to form a more or less "planar" surface out of the particles. Hereby, the preparation of a fixed particle layer at a double–face adhesive tape was selected [11,12]. Contact angle measurements were conducted, using the Wilhelmy method [13], because in sessile drop experiments problems in droplet stability occurred, due to drainage of the drop into the porous particle layer for hydrophilic powders. Before the measurements the adhesive tape was immersed in the filler powder and gently moved, until the tape was uniformly coated by filler particles. Surplus particles, which did not stick at the adhesive tape, were blown away by a stream of nitrogen. Environmental electron microscopy pictures (Fig. 2) show that the – as expected, rather rough – particle coated surfaces are fully covered by filler particles.

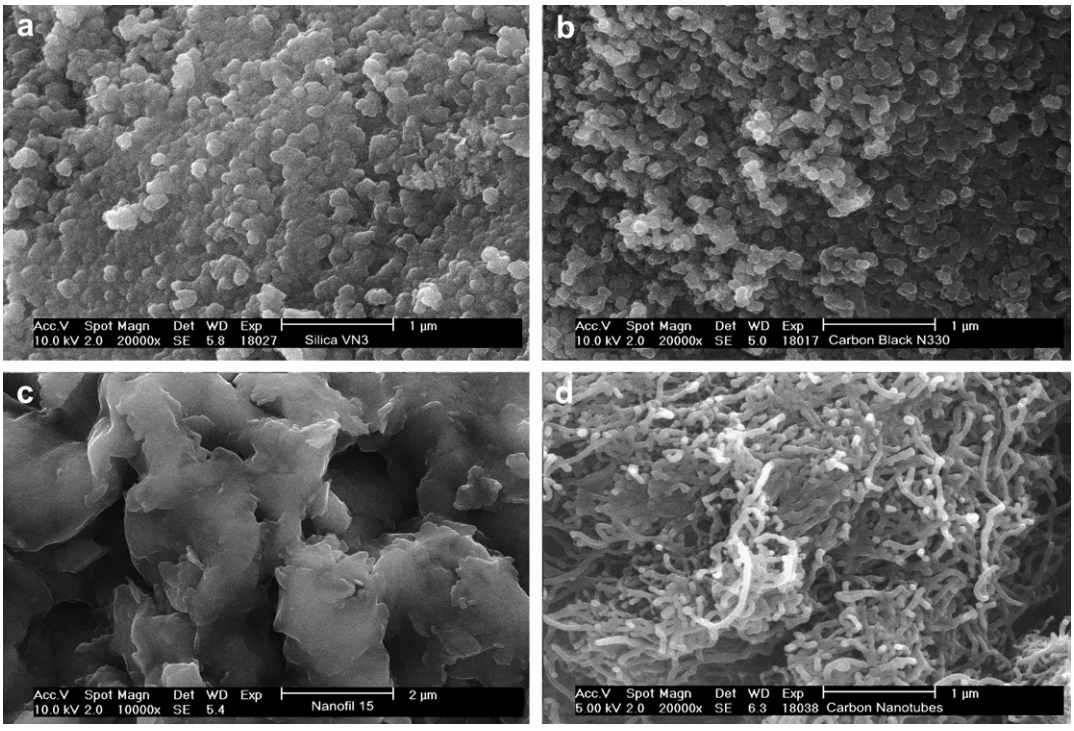

Fig. 2. ESEM-pictures of the filler particle coated adhesive tape of the four main filler types: a) Silica, b) Carbon Black, c) layered Silicates and d) Carbon Nanotubes.

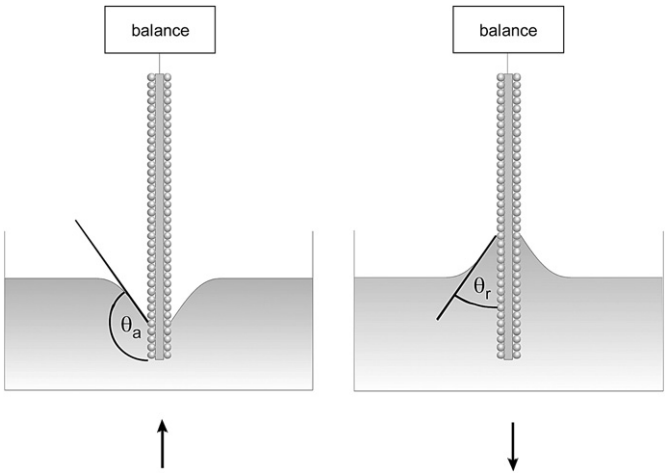

Fig. 3. Schematic representation of the Wilhelmy technique of dynamic contact angle measurement on a particle covered plate. During immersion of the plate the advancing θ_a, during withdrawal the receding contact angle θ_r is measured.

The in this way prepared particle coated plate was attached at the DCAT 21 and the contact angle was measured. For comparison also the native uncovered adhesive tape was analyzed. Hereby, no influence of the supporting tape on the measured contact angles was detected. Furthermore, in the electron microscopic pictures (see Fig. 2) no areas in the particle covered tapes could be found, where an uncovered part of the adhesive tape was visible. To proof, if a component of the adhesive tape or of the attached filler particles is contaminating the test liquids, before and after all measurements the surface tension of the liquid used was controlled by means of a Wilhelmy plate of roughened platinum. In the case that the difference in surface tension before and after the contact angle measurement was exceeding 1 mN/m, the values were not used for an evaluation of surface energies. The contact angles were calculated out of the Wilhelmy measurements (the experimental setup is shown in Fig. 3), using the equation.

$$F = \gamma \cdot \cos(\theta) \cdot l - B \tag{3}$$

hereby, F is the measured force, γ the surface tension of the test liquid, l the wetted length (in this case the circumference of the Wilhelmy plate) and B the buoyancy of the Wilhelmy plate, which was eliminated from the measurement by linear regression of the constant slope of the weight curve, after a constant meniscus between liquid and plate was established Fig. 4.

The dynamic Wilhelmy method yields the advancing contact angle during immersion of the particle covered plate, and the receding angle during withdrawal out of the test liquid. Expectedly, the intrinsic roughness and/or heterogeneity of the particle layers cause in some measurements a high contact angle hysteresis, in extreme case up to a jump in ultrahydrophobic behaviour ($\cos(\theta) \rightarrow -1$) or total wetting ($\cos(\theta) \rightarrow 1$). Nevertheless, it was possible to measure contact angles on all filler particle systems with a number of different test liquids, to obtain an experimental basis for a calculation of surface energies of these granular matters.

3.1.2. Contact angle measurements of uncured rubber polymers

For an evaluation of the dispersibility of nanoscale filler particles in rubbers, additionally to the surface energetic properties of the filler particles also knowledge of the surface tension of the polymer matrix is necessary. Unlike thermoplastics, even uncured rubber polymers can not be melted. Therefore, most of the methods for characterisation of the measurement of surface tension and polarity of polymers, i.e. axisymmetric drop shape analysis of the melt, can not been used. For this reason, plates of the uncured rubber polymers were prepared in a hot press at 160 °C with a press force of 100 kN using a mould having a PTFE surface to minimize surface contamination of the rubber samples. Some polymer samples showed after this preparation a typical rippling pattern at the surface, which made the contact angle measurement more complicated, but not impossible. Contact angle measurement at the polymer samples were conducted using the sessile drop method and the Wilhelmy method as well. Hereby, the surface tension of the test liquid was checked before and after every measurement, to check a contamination of the liquid and a possible solubility of the polymer in the liquid. If a change in the surface tension of the liquid was observed, the measurements were not taken into account for surface energy evaluation.

3.2. Calculation of surface energies and polarities

It is a matter of common knowledge that no exact algorithm exists for calculating the surface energy of a solid surface from the contact angle data. Nevertheless - or just therefore, a number of semi-empirical methods are in use for evaluation of the surface energy of a solid from wetting measurements. Most of these methods require contact angle measurements with a set of liquids of different surface tensions and polarities. One exception hereby is Neumann's equation of state [14]:

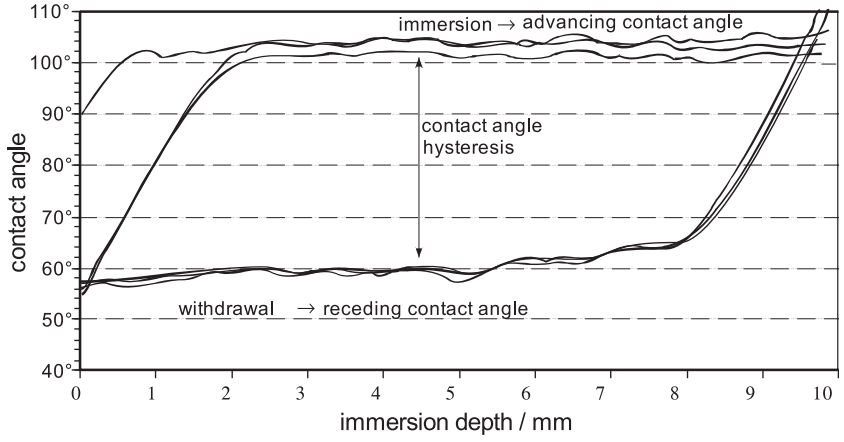

Fig. 4. Typical example of a Wilhelmy measurement curve with buoyancy correction (3 immersion cycles).

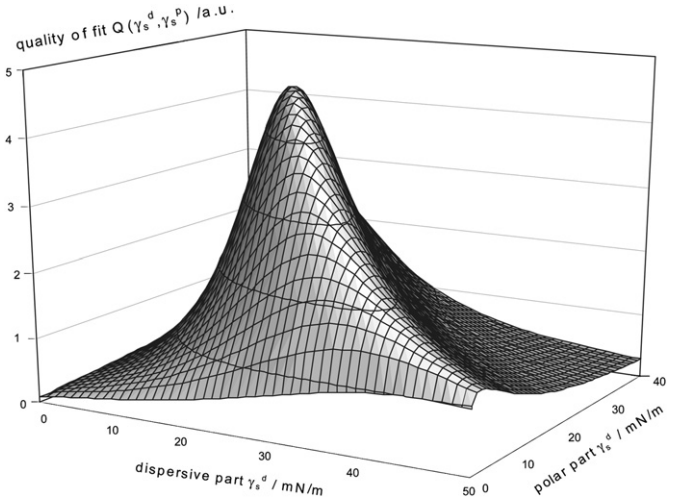

Fig. 5. Plot of the reciprocal value of the sum of the quadratic deviations between the measured and the fitted values ("quality of fit"), using the example of fumed silica (Aerosil 200).

$$\cos\theta = -1 + 2\sqrt{\frac{\gamma_s}{\gamma_l}}\cdot\exp\left(-\beta\cdot(\gamma_l-\gamma_s)^2\right) \quad (4)$$

(with the empiric determined fit factor $\beta = 0{,}0001247$ $(m^2/mJ)^2$), which is able to calculate a surface energy of a solid from one single contact angle measurement. This method was tested with the contact angle data obtained (see Fig. 6), but due to a high scattering of the experimental contact angle values, caused by the intrinsic roughness and heterogeneity of the samples, only the average over several different measurements with different test liquids gave reliable surface energy values. Therefore, it was not possible, to reduce the experimental effort by using Neumann's algorithm.

Several methods (particularly Fowkes [15] or Owens and Kaelble [16,17]) split the surface tensions and energies of liquids and solids in a polar and a dispersive part. Hereby, the dispersive part represents the interactions due to London's dispersion forces; the polar part subsumes the interactions, which are evoked by polar functional groups, i.e. hydroxy, carboxyl or amino moieties. The dispersive and the polar part add up to the total surface energy:

$$\gamma = \gamma^d + \gamma^p \quad (5)$$

the relation of contact angle and disperse and polar part of the surface energies of the solid (γ_s) and liquid (γ_l) phases was given by Fowkes [15] as:

$$\cos\theta = -1 + \frac{2\sqrt{\gamma_s^d\gamma_l^d}}{\gamma_l} + \frac{2\sqrt{\gamma_s^p\gamma_l^p}}{\gamma_l} \quad (6)$$

From the several algorithms for evaluating the surface energy of a solid surface from equation (6), the fitting procedure according Wicks and Clint [18] was chosen, due to its robustness and good stability. Surface energy values were calculated for all contact angles measured: in the case of a fixed filler particle layer for advancing, receding contact angles obtained by the Wilhelmy method and their mean; for the rubber polymers additionally from sessile drop measurements. A "quality of fit" – plot (Fig. 5 acc. [18]), which depicts the reciprocal value of the sum of the quadratic deviations for a set of combinations of polar and dispersive parts of the surface energy of the solid surface shows the robust fitting method by a sharp single maximum.

The Tables 1 and 2 show the surface energy values of the filler systems and the rubber polymers, calculated by fitting of Fowkes' equation out of the advancing, receding and the mean values of the contact angles, measured by the Wilhelmy method. For the rubber polymers also values calculated from sessile drop contact angles are given (Table 2). Using the dynamic Wilhelmy method for contact angle measurement good reproducible advancing and receding contact angles can be obtained. For an evaluation of the equilibrium or Young's contact angle from dynamic contact angles no common accepted analytical method is known. Recent publications [19,20] assume that between the measured advancing and receding contact angle of a system a multiplicity of meta-stable states is present. Because there is no method to find out the absolute energetic minimum of the system, mostly the arithmetic mean of the advancing and receding angle is used, as we do in the prevailing paper.

From all contact angle data also surface energy values were calculated, using Neumann's equation of state. Fig. 6 shows a comparison of the arithmetic mean of surface energy values of the fillers obtained by Neumann's equation (4) for the set of 7 test liquids and the result of a fit of Fowkes' equation (6). It is observable that for low energetic surfaces the values are rather similar; for high energetic (or more polar) surfaces the deviation between the two methods is increasing. Since Fowkes' evaluation delivers the polar and the dispersive part of the measured surface energies, which are

Table 1
Surface energy values of different filler systems.

filler type	Wilhelmy method advancing contact angle				Wilhelmy method receding contact angle				Wilhelmy method mean contact angle			
	γ_s^d mJ/m^2	γ_s^p mJ/m^2	γ_s mJ/m^2	P %	γ_s^d mJ/m^2	γ_s^p mJ/m^2	γ_s mJ/m^2	P %	γ_s^d mJ/m^2	γ_s^p mJ/m^2	γ_s mJ/m^2	P %
TESA 55377[a]	21.4	0.0	21.4	0.0	18.8	22.9	41.6	54.9	22.4	4.7	27.1	17.4
Silica VN3 pulv.	21.5	5.5	27.0	20.2	17.9	29.7	47.6	62.4	19.4	18.9	38.3	49.4
Silica VN3 gran.	20.2	11.9	32.1	37.0	17.7	30.0	47.8	62.9	18.7	22.7	41.3	54.8
Coupsil 8113 pulv.	27.5	0.0	27.5	0.0	17.0	33.5	50.5	66.4	22.2	10.8	32.9	32.7
Coupsil 8113 gran.	28.2	1.1	29.3	3.8	17.2	33.0	50.1	65.8	21.1	15.8	36.9	42.9
Aerosil 200	26.3	0.5	26.7	1.8	17.0	33.9	51.0	66.5	20.0	17.3	37.3	46.4
Aerosil R974	18.8	0.0	18.8	0.0	18.8	0.0	18.8	0.0	13.1	0.0	13.1	0.0
CB N121	21.6	0.0	21.6	0.0	33.0	0.0	33.0	0.0	28.1	0.0	28.1	0.0
CB N234	30.4	0.0	30.4	0.0	25.9	5.9	31.8	18.6	29.5	1.1	30.6	3.7
CB N339	22.0	0.0	22.0	0.0	31.3	0.0	31.3	0.0	27.0	0.0	27.0	0.0
CB N990	18.2	0.0	18.2	0.0	19.1	23.9	43.0	55.5	26.8	0.7	27.5	2.5
MWCNT	23.5	0.0	23.5	0.0	29.9	1.7	31.7	5.5	30.9	0.0	30.9	0.1
MWCNT-OH	24.1	0.0	24.1	0.0	29.4	2.2	31.6	6.8	31.1	0.0	31.1	0.0
MWCNT-SH	23.5	0.0	23.5	0.0	27.9	3.9	31.8	12.2	30.4	0.0	30.4	0.0
Nanofil 757	18.5	23.8	42.3	56.2	17.1	33.7	50.8	66.4	17.5	30.6	48.2	63.6
Nanofil 5	14.6	0.0	14.6	0.0	17.6	30.4	48.0	63.4	22.8	2.4	25.2	9.5
Nanofil 15	12.6	0.0	12.6	0.0	17.8	30.4	48.2	63.0	24.3	1.0	25.3	4.1

[a] Supporting adhesive tape for comparison.

Table 2
Surface energy values of different rubber polymers.

rubber polymer	sessile drop contact angle				Wilhelmy method advancing contact angle				Wilhelmy method receding contact angle				Wilhelmy method mean contact angle			
	γ_s^d mJ/m^2	γ_s^p mJ/m^2	γ_s mJ/m^2	P %	γ_s^d mJ/m^2	γ_s^p mJ/m^2	γ_s mJ/m^2	P %	γ_s^d mJ/m^2	γ_s^p mJ/m^2	γ_s mJ/m^2	P %	γ_s^d mJ/m^2	γ_s^p mJ/m^2	γ_s mJ/m^2	P %
HNBR	22.3	2.8	25.1	11.0	19.5	0.8	20.3	3.7	21.9	17.4	39.4	44.3	21.0	7.4	28.4	26.2
EPDM	24.2	2.9	27.2	10.8	23.7	1.1	24.8	4.3	22.8	18.7	41.4	45.0	24.2	7.6	31.7	23.8
BR	18.4	3.7	22.1	16.8	22.9	0.5	23.4	2.1	21.9	19.8	41.6	47.5	21.5	9.7	31.1	31.0
NBR2	18.6	5.9	24.5	24.1	22.4	0.0	22.4	0.0	23.4	13.0	36.4	35.7	24.1	3.1	27.2	11.3
NBR1	18.9	6.3	25.2	24.8	17.8	0.6	18.4	3.4	22.2	14.9	37.1	40.1	20.8	6.1	26.9	22.7
NR	15.9	6.1	22.1	27.8	17.5	2.4	20.0	12.1	23.4	6.4	29.8	21.3	23.4	6.4	29.8	21.3
NBR3	23.5	8.6	32.1	26.9	24.5	0.0	24.5	0.0	22.2	15.2	37.5	40.6	22.6	5.3	27.9	18.9
CR	19.3	23.7	43.0	55.1	23.3	4.9	28.2	17.5	22.4	19.4	41.8	46.5	22.5	12.2	34.7	35.2
XNBR	17.1	33.3	50.4	66.1	21.6	7.1	28.7	24.8	22.3	20.2	42.5	47.5	22.1	14.0	36.0	38.8

useful parameters for calculations of dispersibility and adhesion parameters, we will use in the following discussion these values.

4. Discussion

4.1. Effect of surface energies and polarities on dispersibility

The dispersion of filler particles in the rubber polymers is the first and most important step in the production of an elastomeric nanocomposite. Besides several parameters of the used processing equipment, for example an internal mixer, and beside the viscosity of the rubber polymers, another very important influencing factor is the physico-chemical compatibility of the filler surface and the rubber polymers. Its influence can be quantified in the free energy of immersion, of the filler in the polymer [21]. The free energy of immersion ΔG_i is defined as the difference of the interfacial energy between the solid filler surface and the circumfluent polymer, γ_{sl}, and the surface energy of the filler particle, γ_s:

$$\Delta G_i = \gamma_{sl} - \gamma_s \tag{7}$$

This definition of the free energy of immersion can be illustrated as the comparison of the energies of the non-wetted and the wetted state of the filler particle (see Fig. 7).

If ΔG_i has a negative value, then the wetting of the particle by the rubber polymer is thermodynamically favoured. Positive values of ΔG_i show that an immersion or dispersion of particles is not a preferred thermodynamic state for this particle/polymer system. Therefore, the free energy of immersion can be considered as a predictor for the contribution of thermodynamics to the dispersibility. In the last chapter was shown, how the surface energy of a system of filler particles can be determined; but, the direct measurement of the interfacial energy γ_{sl} is not possible. In combination with Young's equation the free energy of immersion can be written as

$$\Delta G_i = -\gamma_l \cos\theta \tag{8}$$

due to the fact that the contact angles of rubber polymers on a filler surfaces are not accessible for direct measurements, equation (8) can further modified by insertion of Fowkes' equation, which leads to:

$$\Delta G_i = \gamma_l - 2\left(\sqrt{\gamma_s^D \gamma_l^D} + \sqrt{\gamma_s^P \gamma_l^P}\right) \tag{9}$$

with the help of this equation the calculation of the free energy of immersion is possible for all combinations of rubber polymers and filler particles, by knowledge of disperse and polar parts of their surface energies (see Tables 1 and 2). Table 3 shows the values of

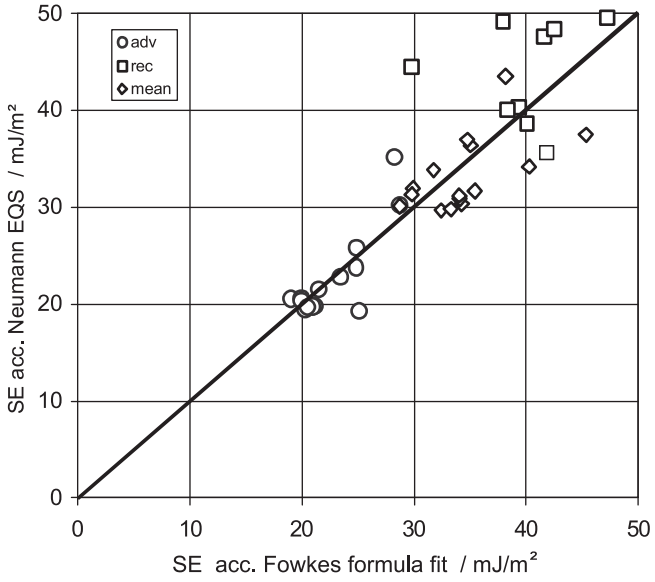

Fig. 6. Comparison of the surface energy values (SE) of the fillers, obtained by the fit of the Fowkes' equation (*x*-axis) with the mean value of surface energies, calculated by Neumann's equation of state (*y*-axis).

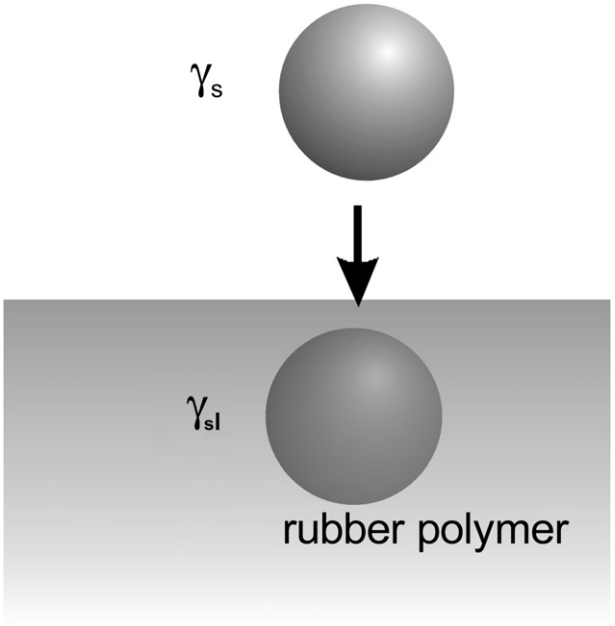

Fig. 7. Schematic representation of the free energy of immersion.

Table 3
Free energy of immersion for the combinations of fillers and rubber polymers, calculated from the surface energies (from sessile drop measurements of the polymers and the mean values of advancing and receding wetting measurements of the Wilhelmy measurements of the fillers) in mJ/m^2.

ΔG_i/mJ/m^2	HNBR	EPDM	BR	NBR2	NBR1	NR	NBR3	CR	XNBR
Silica VN3 pulv.	−31.0	−31.0	−32.4	−34.6	−34.9	−34.6	−36.1	−38.0	−36.2
Silica VN3 gran.	−31.7	−31.7	−33.3	−35.9	−36.3	−36.0	−37.8	−41.4	−40.4
Coupsil 8113 pulv.	−30.4	−30.4	−31.0	−32.1	−32.3	−31.8	−32.9	−30.4	−26.5
Coupsil 8113 gran.	−31.6	−31.6	−32.6	−34.4	−34.7	−34.3	−35.7	−36.1	−33.5
Aerosil 200	−31.1	−31.1	−32.3	−34.3	−34.6	−34.2	−35.7	−36.8	−34.6
Aerosil R974	−9.1	−8.5	−9.0	−6.7	−6.3	−6.9	−3.0	11.2	20.5
CB N121	−25.0	−25.1	−23.4	−21.2	−20.9	−20.3	−19.3	−3.6	6.6
CB N234	−29.7	−29.9	−28.5	−27.4	−27.3	−26.5	−26.7	−14.9	−6.6
CB N339	−24.0	−24.0	−22.5	−20.3	−20.0	−19.4	−18.3	−2.7	7.4
CB N990	−26.6	−26.7	−25.5	−24.2	−24.0	−23.4	−23.0	−10.6	−2.1
MWCNT	−27.4	−27.6	−25.6	−23.4	−23.1	−22.3	−21.8	−5.8	4.4
MWCNT-OH	−27.6	−27.8	−25.7	−23.6	−23.3	−22.5	−22.0	−6.0	4.3
MWCNT-SH	−27.0	−27.1	−25.2	−23.1	−22.7	−22.0	−21.4	−5.4	4.8
Nanofil 757	−32.9	−32.9	−35.1	−38.5	−38.9	−38.7	−40.9	−47.6	−48.0
Nanofil 5	−25.2	−25.2	−24.8	−24.2	−24.1	−23.7	−23.3	−14.0	−7.0
Nanofil 15	−24.8	−24.8	−24.0	−22.9	−22.7	−22.3	−21.6	−10.0	−1.9

ΔG_i derived from the mean surface energy values of the Wilhelmy wetting experiments.

Fig. 8 displays that two groups of fillers can be identified when plotting the free energy of immersion versus the polar part of the surface energy of the examined rubber polymers. The first group shows a decreasing ΔG_i-value at increasing polymer polarity and contains all filler particles with polar surfaces (unmodified silica, unmodified layered silicate).

The second group, containing all filler systems with non-polar surfaces (i.e. carbon blacks, carbon nanotubes, methylated silica, and organophilic modified clays) shows the opposite behaviour. In this case, the free energy of immersion increases with increasing polarity of the rubber, which means that a dispersion of these fillers is not favoured in a polar polymer matrix.

Silica, pre-treated with a sulphur-containing silane (Coupsil 8113), shows the lowest dependency from the polarity of the polymer; whereas the methylated silica Aerosil R974 exhibits the strongest dependency from the polarity of the rubber and can, due to the positive ΔG_i values, hardly be wetted by polar rubbers like XNBR or CR.

It has to be emphasised that the free energy of immersion reflects hereby only the thermodynamic contribution of the wetting of the filler particles by the rubber polymer and delivers one important parameter for the dispersion process, but does not contain the contribution of the mechanical energy of mixing. A filler will be dispersed in a rubber polymer much easier, if the wetting of the filler particles by the polymer is thermodynamically favoured, which is expressed by a highly negative ΔG_i-value.

4.2. Adhesion between filler particles and polymer matrix

Strongly connected with the free energy of immersion is the work of adhesion between filler surface and polymer matrix W_a, which is also determined by the wetting process of the filler surface and the polymer. The work of adhesion between a solid and a liquid phase is defined by:

$$\Delta W_a = \gamma_s + \gamma_l - \gamma_{sl} \tag{10}$$

and can be interpreted as the work, which has to be applied to separate two phases, which are already in contact. By combination of equation 10 with Young's equation, the well known Young–Dupré equation for the work of adhesion is given:

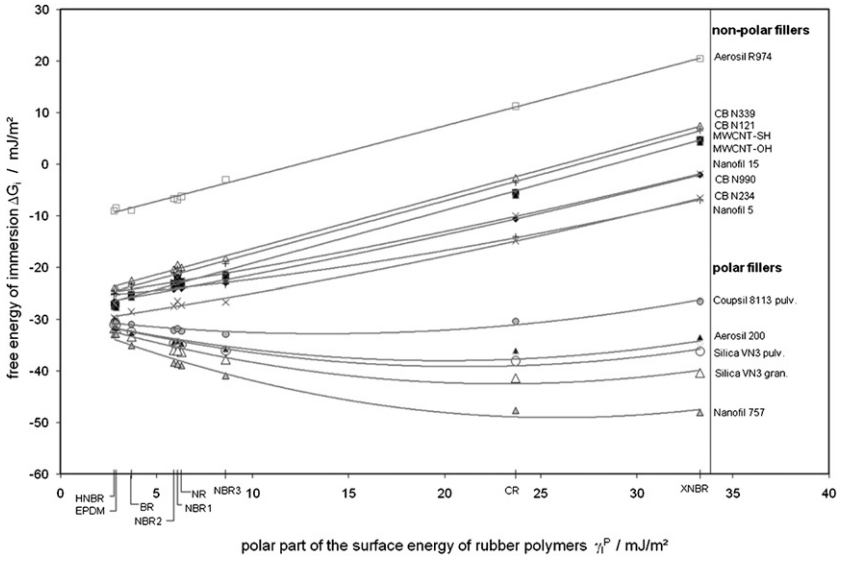

Fig. 8. Free energy of immersion of different filler/rubber combinations, plotted versus the polar part of the surface energy of the rubber polymers γ_l^P.

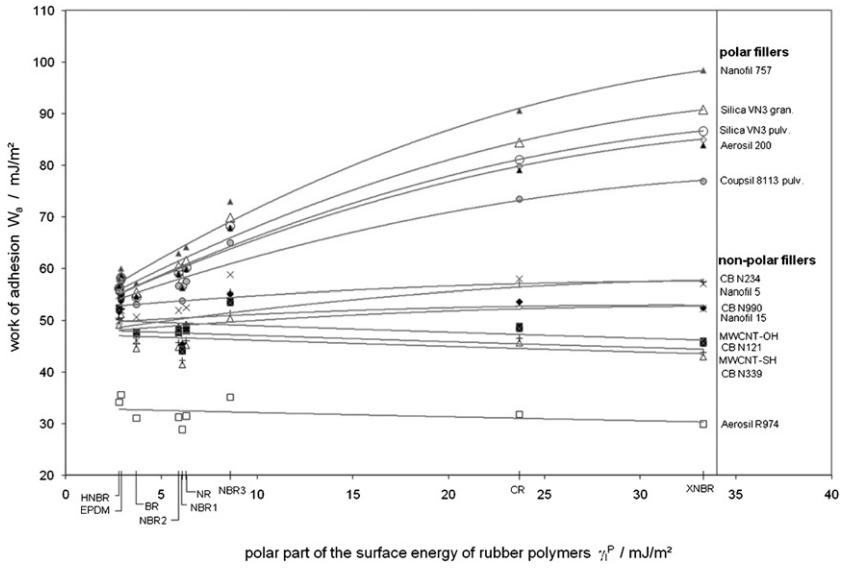

Fig. 9. Work of adhesion of different filler/rubber combinations, plotted versus the polar part of the surface energy of the rubber polymers γ_l^P.

$$W_a = \gamma_l(1+\cos\theta) \tag{11}$$

in the Young–Dupré-equation (11) the correlation of wetting and adhesion is easily demonstrated: for total wetting (contact angle $\theta = 0°$) the work of adhesion is equal $2\gamma_l$, which can also be interpreted as work of cohesion in one single phase. In the other extreme case of non-wetting ($\theta \rightarrow 180°$) the work of adhesion drops towards zero.

Owing to the high viscosity of rubber polymers and having no molten state the contact angle of rubber on filler materials is not measurable. Therefore, the Young–Dupré equation is reformulated by insertion of equation. 6, which leads to

$$W_a = 2\left(\sqrt{\gamma_s^D\gamma_l^D} + \sqrt{\gamma_s^P\gamma_l^P}\right) \tag{12}$$

equation 12 shows the close connection of the work of adhesion with the free energy of immersion by the relation:

$$\Delta G_i = \gamma_l - W_a \tag{13}$$

As it can bee seen in Fig. 9, the work of adhesion is dependent from the polarity of the rubber material. The value of W_a is increasing, when the polar part of the surface energies of both rubber and polymer is increasing, as predicted by equation 12. The filler systems can be distinguished in two classes: “polar fillers”, where the work of adhesion shows a strong dependency on the polar part of the surface tension of the polymer matrix; and the group of the “non-polar” fillers, where the W_a is nearly independent of the of polymer polarity. This is a consequence of equation 12, in which only the interactions of the always present dispersive parts of the surface energies of polymer and filler with each other and the interaction of the highly variable polar parts of the surface energies with each other give a contribution to the work of adhesion. The methylated silica Aerosil R974 for example shows the poorest adhesion to all kinds of rubbers, because of its totally missing surface polarity.

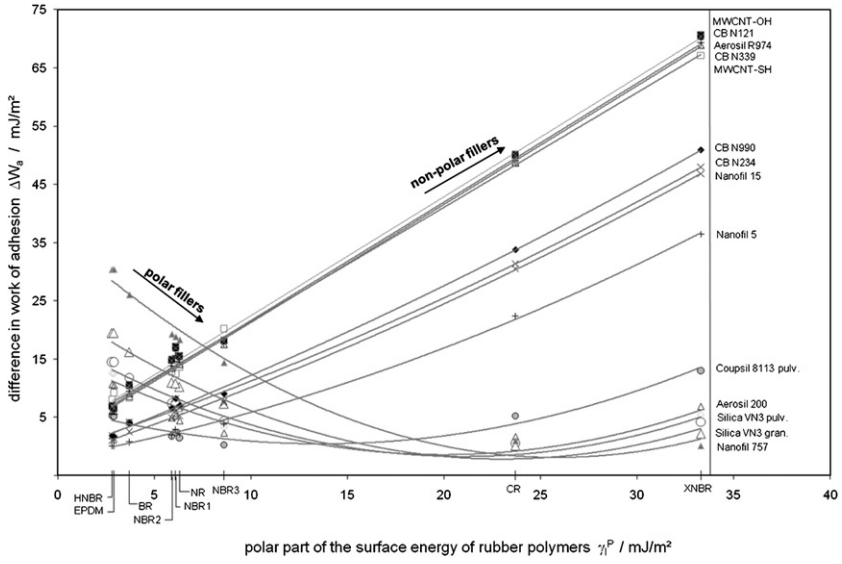

Fig. 10. The difference of Work of adhesion ΔW_a of different filler/rubber combinations as a function of the polar part of the surface energy of the rubber polymers γ_l^P.

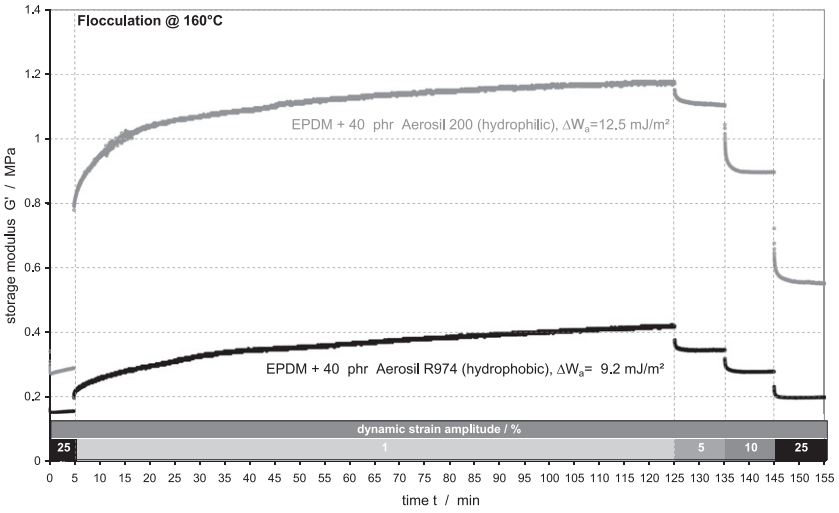

Fig. 11. Flocculation experiment of two types of fumed silicas in EPDM (without addition of curing chemicals), differing only in the modification of the filler surface.

4.3. Influence of surface properties on filler flocculation

The re-agglomeration of dispersed filler particles in the polymer matrix has a crucial influence on the final properties final of rubber products. It is well known that some fillers are forming an expanded network in the rubber matrix in a process called filler flocculation [22,23]. These filler networks influence the dynamic-mechanical properties of the elastomeric material and are considered to be the reason of the amplitude dependency of the elastic storage modulus of filled rubbers, the so-called Payne–effect. Wang [7,24] pointed out that the tendency of filler particles to flocculate is thermodynamically driven by the difference in the work of adhesion between the state of a filler particle in contact with polymer and the flocculated state, where the filler particles are in contact with each other. He formulated the following equation for this difference in work of adhesion ΔW_a:

$$\Delta W_a = W_a(\mathrm{FF}) + W_a(\mathrm{PP}) - 2\cdot W_a(\mathrm{FP}) \tag{14}$$

where W_a(FF) means the work of adhesion of two filler particles and W_a(PP) and W_a(FP) between the polymers and filler and polymer, respectively.

After inserting the terms for the work of adhesion according equation 12, we derive after some rearranging the relation:

$$\Delta W_a = 2\cdot\left(\sqrt{\gamma_F^D} - \sqrt{\gamma_P^D}\right)^2 + 2\cdot\left(\sqrt{\gamma_F^P} - \sqrt{\gamma_P^P}\right)^2 \tag{15}$$

The difference of work of adhesion ΔW_a tends to zero, when the polar and the disperse part of the surface energies of filler and polymer matrix are equal. This has the consequence that filler particles, which have the same interface properties like the surrounding polymer phase do not tend to flocculate; the bigger the difference of the components of the surface energies of filler and polymer are, the higher is the thermodynamic driving force of the filler particles to flocculate. Therefore, a surface modification of the filler particles can suppress the tendency of filler flocculation in a rubber mixture. In Fig. 10 the difference of work of adhesion is shown for a set of filler/rubber combinations.

Fig. 10 shows also the tendency of flocculation for different filler/rubber combination. Two types of fillers are clearly distinguishable with respect to their flocculation tendency: the polar fillers exhibit decreasing ΔW_a values with increasing polarity of the rubbers, whereas non-polar fillers will tend to flocculate more in a polar filler matrix.

A rheometric study, using a rubber process analyzer (Scarbaeus, Langgöns, Germany) shows the flocculation behaviour of two fumed silicas with the same particle size but different in the surface

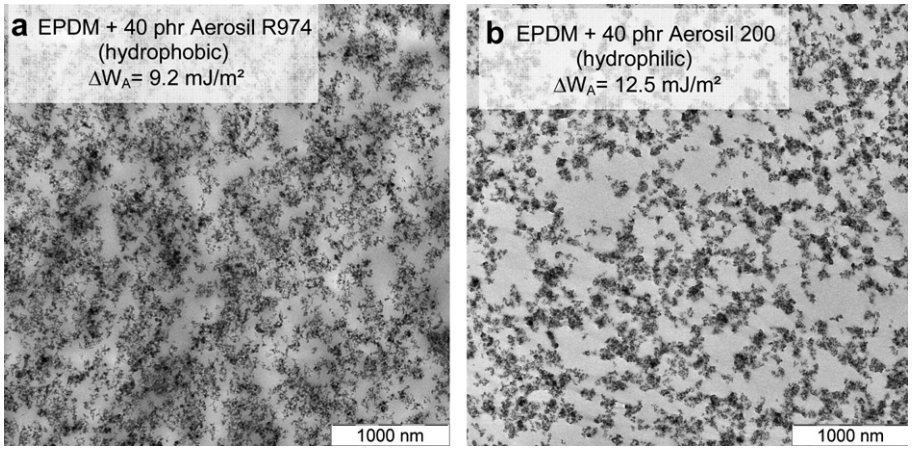

Fig. 12. Transmission electron microscopic images of the flocculation of two types of fumed silicas in peroxide cured EPDM, the difference of the work of adhesion between filler and polymer ΔW_A leads to completely different flocculation behaviour.

treatment – the hydrophilic Aerosil 200 and the methylated silica type Aerosil R974. Mixtures of 40 phr of these silica types in EPDM were prepared without an addition of curatives and measured in the moving die rheometer: After a conditioning step at a high strain amplitude of 25% to destroy a possibly pre-existing filler network, the storage modulus G′ was recorded for 2 h at a low strain amplitude of 1% at 160 °C to observe a filler flocculation. Subsequently, the strain was increased again in tree steps to 5%, 10% and again 25%.

In Fig. 11 the influence of the surface energies on the process of filler flocculation is clearly observable: the hydrophilic silica Aerosil 200, which has a difference of work of adhesion of $\Delta W_a = 12.5$ mJ/m^2 to the EPDM-matrix, exhibits a much higher increase of the storage modulus G' in the flocculation experiment, than the methylated silica type Aerosil R972, with a calculated ΔW_a-value of 9.2 mJ/m^2.

The effect of the influence of different surface energies of the filler surface can also be monitored by transmission electron micrographs (Fig. 12): The methylated fumed silica (Fig. 12a: Aerosil R974) shows a significantly lower flocculation tendency compared with the native silica (Fig. 12b: Aerosil 200), which shows a typical chain-like flocculation structure.

This findings show the crucial effect of the surface energy on the formation of filler networks in elastomers, witch has as consequence impact on the dynamic-mechanic properties of the rubber product.

5. Conclusion

The measurement of surface energies of granular mater, like nanoscale filler particles, is still a challenging and difficult task with several experimental problems due to the irregular size and surface roughness of the particles. Our measurements of surface energies, using the Wilhelmy technique at a layer of particles fixed at an adhesive tape, give a series of relatively good reproducible dynamic contact angles without the experimental problems of swelling, gelation and de-agglomeration in the particle bed, that occur with the Washburn method. We do not claim that the surface energies calculated out of these measurements are absolute values. But, inside the same experimental method, our experiments yield a valuable tool for classification of the different filler systems with respect to their surface energy and polarity. In combination with surface energetic properties of the rubber polymers, also obtained by corresponding wetting measurements, we derived useful thermodynamic parameters for an assessment of dispersibility, adhesion and flocculation behaviour of elastomeric nanocomposites. We feel confident that these thermodynamic parameters may improve considerably the compounding process of novel rubber nanocomposites with respect to target-oriented adjustment of rubber properties.

Acknowledgements

Financial support by the German Federal Ministry of Education and Research BMBF (Grant 03X0002E) and the German Research Council DFG SPP1369 Priority Program are gratefully acknowledged. The authors thank Dr. G. Schmidt (IKGB, TU BA Freiberg) for the ESEM micrographs, Mrs. U. Reuther for the TEM images and Mr. R. Kluge for conducting a great amount of wetting measurements.

References

[1] Heinrich G, Klüppel M, Vilgis T. Reinforced elastomers: from molecular physics to industrial applications. In: Bhowmick Anil K, editor. Current topics on elastomers research. Taylor & Francis; 2008. p. 607–23 [Chap. 22].
[2] Wagenknecht U, Kretzschmar B, Pötschke P, Costa FR, Pegel S, Stöckelhuber KW, et al. Chemie Ingenieur Technik 2008;80(11):1683–99.
[3] Das A, Stöckelhuber KW, Jurk R, Saphiannikova M, Fritzsche J, Lorenz H, et al. Polymer 2008;49:5276–83.
[4] Das A, Jurk R, Stöckelhuber KW, Engelhardt Th, Fritzsche J, Klüppel M, et al. J Macrom Sci Part A: Pure and Appl Chem 2008;45(2):144–50.
[5] Kohjiya S, Ikeda Y. Rubber Chem Technol 2000;73(3):534–50.
[6] Payne AR. J Appl Polym Sci 1962;6:57–62.
[7] Wang M-J. Rubber Chem Technol 1998;71:520–89.
[8] Pepin X, Blanchon S, Couarraze G. Pharm Sci TechnToday 1999;2(3):111–7.
[9] Lucas R, Kolloid Z. 1918;23:15–22.
[10] Washburn EW. Phys Rev 1921;17:273–83.
[11] Bachmann J, Horton R, van der Ploeg RR, Woche S. Soil Sci Soc Am J 2000;64:564–7.
[12] Kvítek L, Pikal P, Kovaříková L, Hrbáč J. Acta Univ Palacki Olomuc Chemica 2002;41:27–35.
[13] Wilhelmy L. Annalen der Physik und Chemie 1864;119:177–217.
[14] Neumann AW, Li D. Adv Colloid Interface Sci 1992;39:299.
[15] Fowkes FM. J Phys Chem 1963;67:2538–41.
[16] Owens DL, Wendt RC. J Appl Polym Sci 1969;13:1741–7.
[17] Kaelble DH. J Adhes 1970;2(2):66–82.
[18] Clint JH, Wicks AC. Int J Adhesion & Adhesives 2001;21:267–73.
[19] Marmur A. Soft Matter 2006;2:12–7.
[20] Long J, Chen P. Adv Colloid Interf Sci 2006;127:55–66.
[21] Rulison C. Two-component surface energy characterization as a predictor of wettability and dispersability, AN213/CR, KRÜSS Application Note#213.
[22] Böhm GGA, Nguyen MN. J Appl Polym Sci 1995;55:1041–50.
[23] Lin CJ, Hergenrother WL, Alexanian E, Böhm GGA. Rubber Chem Tech 2002;75:865–90.
[24] Wang M.J.KGK. 2007;60:438–43.